

# Novel gelled fuels containing nanoparticles as hypergolic bipropellants with HTP

*Sophie Ricker<sup>1\*</sup>, Maxim Kurilov<sup>1</sup>, Dominic Freudenmann<sup>1</sup>, Christoph Kirchberger<sup>1</sup>, Tobias Hertel<sup>2</sup>, Helmut Ciezki<sup>1</sup> and Stefan Schleichriem<sup>1</sup>*

*<sup>1</sup>DLR, German Aerospace Center, Institute of Space Propulsion, Lampoldshausen, Langer Grund, 74239 Hardthausen, Germany*

*\*Corresponding author: [sophie.ricker@dlr.de](mailto:sophie.ricker@dlr.de)*

*<sup>2</sup>Institute of Physical and Theoretical Chemistry, Julius Maximilian University Würzburg, 97074 Würzburg, Germany*

## Abstract

With the aim of replacing toxic, carcinogenic propellants, new gelled bipropellants were developed. Transition metal based nanoparticles were utilised as new catalysts for the hypergolic bipropellant system with HTP as oxidiser and TMEDA as fuel. To test the quality, ignition delay times (IDTs) were determined via drop-on-pool tests. Various parameters were optimised in order to exploit catalytic activity of the nanoparticles. It was found that silver is most suitable and that size, stabilisation and distribution of the nanoparticles are important. An optimised bipropellant was created which reached an average IDT of  $8.8 \text{ ms} \pm 1.0 \text{ ms}$ .

## 1. Introduction

Hypergolic propellants are commonly used in space flights for many years. They consist of two components – an oxidiser and a fuel – which ignite immediately on contact. Advantages of these fuel combinations are the omission of a separate ignition device as well as the fact, that ignition takes place reliably. The currently most popular hypergolic propellants consist of hydrazine or its derivatives and dinitrogen tetroxide. These substances are categorized as toxic, carcinogenic and environmentally problematic; therefore the handling of these substances is rather difficult as complex safety equipment is indispensable. In 2011, hydrazine was added to the list of substances of very high concern by Europe's REACH regulation (Registration, Evaluation, Authorization and restriction of Chemicals). For these reasons, a lot of research on new, less toxic "green propellants" is done. Hypergolic propellants are often used, when the mission requires reliable and repeated ignition. The main application areas are satellites, manned spacecraft, space stations and probes. [1-3].

The hurdle in the development of green propellants is to obtain similar performance figures as in commonly used hypergolic fuels. One approach for such alternative propellant candidates is the use of gelled, hypergolic fuels with HTP (high test peroxide) as oxidiser. In this paper we focused on the ignition delay time (IDT) as performance parameter of the hypergolic propellants. A short IDT is very interesting due to different aspects, for example when several engine or thruster firings need to be carried out in a short time. Longer IDTs can lead to propellant accumulation and therefore to an uncontrolled ignition or even a disastrous hard start [4,5]. For the hypergolicisation of propellants with HTP, suitable additives must be added to the fuel. So far, metal salts or metal hydrides are utilised often. This work focuses on the new idea of transition metal nanoparticles as catalysts for hypergolic bipropellants with HTP.

### 1.1 Gelled Propellants

Gels are homogenous mixtures of liquids with suitable gelling agents. Due to their non-Newtonian flow behaviour they act like solids when stored in the tank, but can be liquefied easily through shear forces. That's the reason why gels are able to combine the advantages of both solid and liquid propulsion systems. On the one hand, an easy thrust regulation is possible similar to liquid propellants. On the other hand, they possess easy usage and storage properties. In our work gelled propellant showed another beneficial property: gelling prevented particles sedimentation. [6]

The selection of a suitable gelling agent depends on the liquid that is used. In this work, the amine TMEDA (*N,N,N',N'*-tetramethylethylenediamine) was used as starting material for the fuels (Fig. 1). Compared to hydrazine and its derivatives, TMEDA shows a significantly decreased toxicity and is therefore an appropriate substance for green propellants. [7] Because of their basicity, amines are suitable fuels with HTP as the oxidiser by nature. Hydrogen peroxide is slightly acidic, therefore the decomposition process of a basic fuel is accelerated, which in turn leads to a faster heat release. [8]

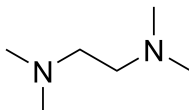


Figure 1: Chemical structure of the molecule TMEDA.

## 1.2 HTP: Characterisation of the oxidiser

Highly concentrated hydrogen peroxide (high test peroxide, HTP), which can be used both, as a monopropellant or as an oxidiser in bipropellant combinations, represents an environmental friendly alternative to commonly used oxidisers like fuming nitric acid, NTO or MON. The contact of HTP with certain organic fuels with suitable additives leads so a self-initiated ignition with IDTs in the millisecond range. [5]

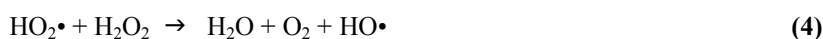
Hydrogen peroxide is a metastable compound which tends to decompose to water and oxygen in an exothermic reaction:



The velocity of this disproportionation is very low under standard conditions. But at higher temperatures, the decomposition takes place rapidly or even explosively. The inhibition of this reaction at room temperature is caused by the first step of the reaction, in which the splitting of the  $\text{H}_2\text{O}_2$  molecule in two hydroxyl radicals takes place. For this process a large amount of energy is required:



Next, a just formed hydroxyl radical reacts with a  $\text{H}_2\text{O}_2$  molecule. Now a chain reaction is started and the rapid decomposition of further hydroxide peroxide molecules proceeds:



The decomposition speed at room temperature can be increased through certain catalysts. As heterogeneous catalysts, potential candidates are materials like silver, gold, platinum or manganese dioxide. [9]

In case of hypergolic bipropellants, HTP is mixed with TMEDA, which contains the catalyst. The released heat of this highly exothermal reaction (see equation 1) leads to the evaporation of the fuel or the heating above its AIT (auto-ignition temperature). When a substance reaches its AIT, it ignites without an additional ignition source with air. This temperature is 145 °C for TMEDA. Out of this mechanism results the fact, that ignition with metal salts or metals as catalysts, is mainly controlled by the time, which is needed for  $\text{H}_2\text{O}_2$  decomposition. [10,11]

## 1.3 Nanoparticles and colloids

This work focuses on transition metal based nanoparticles as catalysts for hypergolic propellants with HTP. Nanoparticles are defined as structures on a scale between approximately 1 nm and 100 nm. Today, nanoparticles are widely used, as they show significant changes in their optical, magnetical, electrical and mechanical properties compared to bulk material. [12] The increased growth of the nanotechnology is illustrated on basis of the number of hits which are obtained by the keyword “nanoparticles” on the SciFinder database since 1990 (Fig. 2).

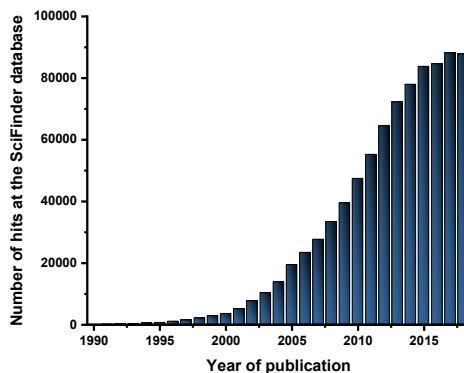


Figure 2: Number of hits which are obtained by the keyword “nanoparticles” on the SciFinder database.

Nanotechnology plays a major role in the field of catalysis, as reactions usually take place at the surface of a material. Nanoparticles distinguish from bulk material notably by their very large surface to volume ratio, so the consequence is a vast increase in reactivity of the nanoparticles.

A colloidal system is a mixture of a finely dispersed liquid or solid in the size range between 1 nm and 1000 nm in a dispersant. Thermodynamic instability of colloidal particles is given by their large specific surface and the related high free enthalpy. The consequence is the possibility of the agglomeration of the particles:

$$dG = \sigma \cdot dA_G \quad (5)$$

Reduction of the interface area  $A_G$  leads to decrease of the free enthalpy  $dG$  of the colloid, whereby the aggregation of the system is benefited. The kinetic stability of the dispersion depends on the interaction of the particles (or bubbles in case a liquid is dispersed) with the dispersant. Attractive interactions like adsorption forces, attractive electrostatic forces or *van der Waals* forces destabilise the colloid, while repulsive interactions like electrostatic repulsion between the particles are counteracting. [13]

The DLVO theory (named after Derjaguin, Landau, Verwey and Overbeek) developed an approach for visualization of the stability of colloidal systems. It is based on the fact, that the surface of dispersed particles is usually charged. In case of former uncharged particles, this is due to the formation of a surface charge by the interaction with the liquid medium. It creates the situation where the ions in the surrounding medium are orientating around the particles. Through the division of the ion envelope into different layers, the shear radius is introduced. This is an inner layer, which involves rigidly arranged ions that move together with the particle in the dispersion (Fig. 3). This layer is responsible for the mobility of the particles; the electric potential at this interface is called zeta potential  $\zeta$ . A high absolute value of the zeta potential indicates a highly repulsive interaction of the particles and therefore a high stability of the colloid. Dispersions with values from about  $\zeta = \pm 30$  mV are classified as electrostatically stable. [14-18]

Stability of a colloid can be increased by sterically demanding ligands. For example through the coverage with polymers that can be adsorbed by the particle surface. Interaction of the polymer chains of two neighbored particles leads to a decrease of their mobility. Consequently the entropy of the whole system decreases, so the approximation of two particles is thermodynamically unfavourable. This type of stabilisation is called *steric stabilisation*. Another kind of stabilisation is *electrostatic stabilisation*. Through the increase of the charge density at the particle surfaces, the potential energy barrier for the flocculation of the particles increases. So the flocculation of the particles is prevented and the colloid is stabilised. When both stabilisation effects are involved, this is called *electrosteric stabilisation*. [18,19]

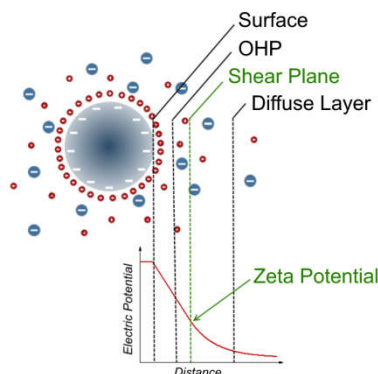


Figure 3: Illustration of the zeta potential on basis of the double layer model. OHP: Outer Helmholtz plane. [20]

## 2. Nanoparticles: selection, synthesis and characterisation

Criteria for the selection of the materials were – beside catalysis of the decomposition of hydrogen peroxide – reduced toxicity and carcinogenicity, environmental friendliness, cost of the nanoparticles or the reactants and easy access to the respective nanoparticles. For these reasons, silver, platinum and manganese dioxide particles were chosen and synthesised in the laboratory via bottom-up synthesis methods. The silver nanoparticles were produced through reduction of silver nitrate ( $\geq 99.9\%$ , Carl Roth) in the presence of capping agents like polyvinylpyrrolidone (PVP, pure, Carl Roth) or sodium citrate ( $> 99\%$ , Carl Roth). Ethylene glycol ( $> 99.5\%$ , Merck), sodium citrate or D-Glucose ( $\geq 99.5\%$ , Sigma) were used as reducing agents. These partially remain as surround of the nanoparticles to provide stabilisation of the colloidal system. Platinum nanoparticles were obtained through reaction of chloroplatinic acid (Carl Roth) with ethylene glycol. Manganese dioxide nanoparticles were synthesized through reaction of manganese sulfate monohydrate (Ph. Eur., Merck) with an aqueous solution of sodium hydroxide ( $> 99\%$ , Merck). All chemicals were used as received. The synthesis procedures were adapted from literature. [21-25]

The nanoparticles were characterised via dynamic light scattering (DLS), UV-Vis spectroscopy and zeta potential measurement. In case of the manganese dioxide particles, also IR and Raman spectroscopy were utilised. In order to identify the amount of the above mentioned capping agents, thermogravimetry (TG) and differential scanning calorimetry (DSC) as well as IR spectroscopy were used. EDX spectroscopy was used to verify the chemical composition and purity of the nanoparticles (Tab. 1).

An interesting aspect of metallic nanoparticles is the *plasmon resonance effect*. It is a useful phenomenon for characterisation of nanoparticles via UV/Vis spectroscopy, as it is dependent on the particle size. In case of silver particles, the absorption maximum is located between 400 nm and 530 nm. With the increase of particle sizes, the absorption maxima show a bathochromic shift. Additionally, larger particle radii are related with a broadening of the absorption band. Particles of a size from about 80 nm or larger show a second absorption band between 350 nm and 450 nm. Figure 4 shows this correlation with the three different kinds of synthesised silver nanoparticles.

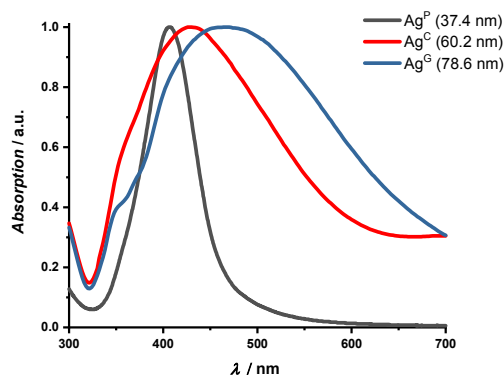


Figure 4: Comparison of the absorption spectra of synthesised silver nanoparticles of different size, which were utilised for the hypergolic bipropellants afterwards. The average size of the particles is indicated (determined by dynamic light scattering).

Table 1: Summary of spectroscopic characterisation of the different nanoparticles. In case of silver, particles of different sizes were synthesised. The abbreviations are derived from the synthesis method that was used respectively.  $\text{Ag}_{\text{nano}}^{\text{C}}$ : silver nanoparticles, synthesised through citrate method;  $\text{Ag}_{\text{nano}}^{\text{G}}$ : silver nanoparticles, synthesised through glucose method;  $\text{Ag}_{\text{nano}}^{\text{P}}$ : silver nanoparticles, synthesised through polyol method.

	$\text{Ag}_{\text{nano}}^{\text{P}}$	$\text{Ag}_{\text{nano}}^{\text{C}}$	$\text{Ag}_{\text{nano}}^{\text{G}}$	$\text{Pt}_{\text{nano}}$	$\text{MnO}_{2(\text{nano})}$
Particle size (DLS) [nm]	$37.4 \pm 10.4^a$	$60.2 \pm 17.9^a$	$78.6 \pm 20.0^a$	$73.5 \pm 20.6^b$	$67.7 \pm 19.3^a$
Absorption maximum (UV/Vis spectroscopy) [nm]	$407^a$	$428^a$	$468^a$	$278^b$	-
Zeta potential $\zeta$ [mV]	$-21.73^a$	$-40.03^a$	$-20.14^a$	$-11.07^b$	-
Capping agent used in synthesis	PVP ( $M_w = 2\,500$ g/mol)	sodium citrate dihydrate	PVP ( $M_w = 40\,000$ g/mol)	PVP ( $M_w = 10\,000$ g/mol)	-
Amount of remaining capping agent (thermo-gravimetry) [wt%]	0.42	30.9	2.61	2.15	-
IR spectroscopy	✓	✓	✓	✓	✓
Raman spectroscopy	-	-	-	-	✓
EDX	✓	✓	✓	✓	✓

<sup>a</sup>measured in  $\text{H}_2\text{O}$ ; <sup>b</sup>measured in EtOH

### 3. Investigation of the fuels via drop tests

#### 3.1 Preparation of the fuel

First, the nanoparticles (1 wt% or 5 wt%) were placed into a glass vessel and TMEDA was added. A dispersion was prepared with the aid of an ultrasonic probe. The mixture was then heated to  $60\text{ }^\circ\text{C}$  while stirring and adding the silica based gelling agent. After ten minutes, the vessel was sealed and stored at a temperature of  $1\text{ }^\circ\text{C}$ . Figure 5 shows the photograph of two silver nanoparticle TMEDA gels.

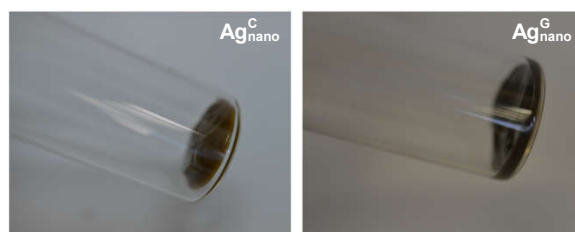


Figure 5: Photographs of two different fuels containing silver nanoparticles. [20]

#### 3.2 Experimental setup

For the measurements of the IDTs, the test setup shown in figure 6 was used. A defined amount of fuel (500 mg to 750 mg) was placed in a glass vessel and set on a laboratory lift. A glass pipette containing HTP was mounted 140 mm above it. The dropping of the hydrogen peroxide was controlled via a syringe, which was attached to a tube.

The amount of the oxidiser was  $45.5 \text{ mg} \pm 1.29 \text{ mg}$  respectively. Furthermore, a quenching device was arranged. In front of the fume hood and beyond an additional protective screen, the experimental procedure was filmed with a high-speed video camera. A LED-lamp behind the laboratory lift provided unique lightening.

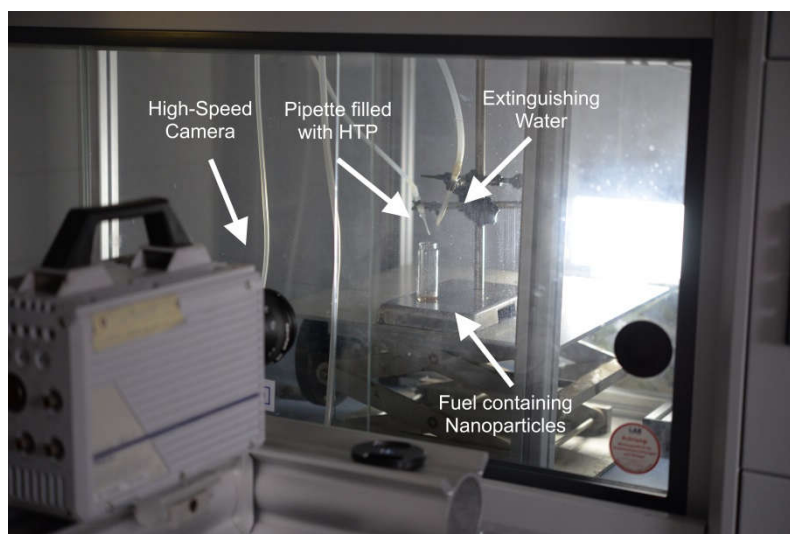


Figure 6: Test setup used for the drop test for the determination of the IDT. [20]

For the examination of different fuels, recorded high-speed videos of the drop tests were analysed frame per frame. The recording speed was 2000 fps or 3000 fps. The IDTs were determined by the sequence between the first contact of fuel and oxidiser and the flame formation. In figure 7, images of the development of a drop-on-pool test are shown. First, the  $\text{H}_2\text{O}_2$  drop approaches the fuel surface. In the next sequence, the first contact of oxidiser and fuel is shown. This is followed by the formation of the flame and its further spread. For every fuel combination, different tests were accomplished. To assess reliability, the standard deviation of the IDTs was determined. As hydrogen peroxide tends to self-decompose, purity of the substance was verified before each test series by measurement of the refractive index. In this way, the hydrogen peroxide contents were determined at  $25 \text{ }^\circ\text{C}$  for the comparison of different test series. All used batches amounted approximately 96 %  $\text{H}_2\text{O}_2$ .

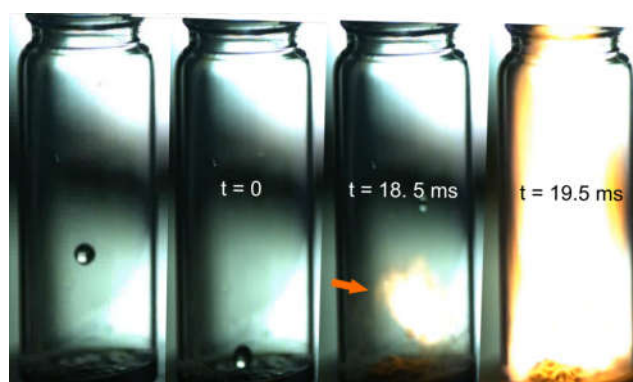


Figure 7: Ignition sequence of propellant containing silver nanoparticles. The IDT in this example is 18.5 ms. [20]

### 3.3 Results and Discussion

Various test series were carried out in order to optimise catalytic functionality of the nanoparticles. Diverse materials were varied step by step to determine the characteristic properties which provide an effective catalysis for the decomposition of hydrogen peroxide. The IDTs which were determined through drop-on-pool tests served as criteria for this decision. The following properties were examined throughout the test series: different materials, size of the nanoparticles, the addition and concentration of stabilising ligands and different ways to introduce the nanoparticles to the fuel (dried or dispersed in ethanol). This work aims to obtain a hypergolic propellant with an IDT as short as

possible. Taking into account that IDTs below 10 ms are considered acceptable for currently used fuel combinations as MMH/NTO or MMH/RFNA, this value was set as benchmark for an ideal case. [7,26]

### 3.3.1 Test series 0: Reference measurement without catalyst

First, the behaviour of the fuel without catalyst was tested for comparing it with the subsequent tests. Therefore a TMEDA gel without nanoparticles was produced and a hypergolicity test with HTP was carried out. The outcome of this analysis was, that even after a long time, no ignition occurred. In the following test series, the influence of additional nanoparticles to the fuel will be tested.

### 3.3.2 Test series 1: Comparison of different nanomaterials

This test series compares three different nanomaterials. The platinum, silver and manganese dioxide nanoparticles were dried and added to the fuel. The amount of the particles in the fuel was 1 wt% respectively. The results of test series 1 are summarised in table 2.

Table 2: Parameters of test series 1 with average IDTs and respective standard deviations.

Catalyst	Average particle size (DLS) [nm]	Amount of catalyst [wt%]	Condition of the nanoparticles	Number of tests	Average IDT [ms]	Standard deviation [ms]
$\text{Pt}_{\text{nano}}$	73.5	1	dried	3	79.2	4.4
$\text{Ag}_{\text{nano}}^{\text{G}}$	78.6	1	dried	3	55.8	3.7
$\text{MnO}_{2(\text{nano})}$	67.7	1	dried	3	148.3	6.4

Analysis of the test data shows, that for the three materials, very different IDTs were determined. The fuels containing manganese oxide nanoparticles show with an average IDT of 148.3 ms  $\pm$  6.4 ms the longest ones by far. About twice as fast, however, are the IDTs which were determined by the platinum nanoparticles containing fuels. The shortest ignition delay times of this test series of 55.8 ms  $\pm$  3.7 ms were measured by the silver nanoparticle containing fuels. For the comparison of the different materials, a uniform size of the different particles would be ideal. Throughout the synthesis of larger amounts of nanoparticles, this optimum couldn't be reached (see table 1). Still, the scales of the nanoparticles are close enough to each other to draw a comparison.

In order to keep sight of the goal – to obtain as short IDTs as possible – the further investigations were carried out with silver nanoparticles only.

### 3.3.3 Test series 2: Effect of the particle size

Now, the influence of different sizes of the nanoparticles was tested in regard to their eligibility as catalyst in the hypergolic propellant. Therefore, silver nanoparticles with three different sizes were synthesised by different methods. The silver nanoparticles were again dried and added to the fuel in a percentage of 1 wt%. The results of test series 2 are collected in table 3.

From these data, no clear tendency regarding the impact of the particle sizes can be made up, as the determined average ignition delay times listed in table 3 are quite similar. The average IDT measured with the fuel containing the smallest nanoparticles was shorter than that with the largest ones, but the shortest average IDT was measured with the fuel containing the medium sized nanoparticles. Considering the standard deviations and measurement uncertainties, it is not possible to make a reliable statement. In test series 3 it will be investigated, whether the previous tendencies are reproducible.

Table 3: Parameters of test series 2 with average IDTs and respective standard deviations.

Catalyst	Average particle size (DLS) [nm]	Amount of catalyst [wt%]	Condition of the nanoparticles	Number of tests	Average IDT [ms]	Standard deviation [ms]
$\text{Ag}_{\text{nano}}^{\text{P}}$	37.4	1	dried	3	47.8	2.3
$\text{Ag}_{\text{nano}}^{\text{C}}$	60.2	1	dried	3	46.3	7.1
$\text{Ag}_{\text{nano}}^{\text{G}}$	78.6	1	dried	3	55.8	3.7

### 3.3.4 Test series 3: Influence of the amount of catalyst

The settings of test series 2 were repeated with the difference, that the amount of the added nanoparticles was increased from 1 wt% to 5 wt%, respectively. On the one hand, the tendencies of the former test series should be rechecked in this way; on the other hand, the impact of the increased amount on catalyst is investigated. The results of test series 3 are listed in table 4:

Table 4: Parameters of test series 3 with average IDTs and respective standard deviations.

Catalyst	Average particle size (DLS) [nm]	Amount of catalyst [wt%]	Condition of the nanoparticles	Number of tests	Average IDT [ms]	Standard deviation [ms]
$\text{Ag}_{\text{nano}}^{\text{P}}$	37.4	5	dried	3	24.7	2.3
$\text{Ag}_{\text{nano}}^{\text{C}}$	60.2	5	dried	3	17.3	0.5
$\text{Ag}_{\text{nano}}^{\text{G}}$	78.6	5	dried	3	51.8	1.4

Test series 3 shows, that the increase of the amount of catalyst leads to significantly shorter IDTs. However, the extend of this effect varies widely between different particles. The data shows, that the propellant containing medium sized silver nanoparticles corresponds to the shortest average IDT (Fig. 8). It is remarkable that the shorter the average IDT with 1 wt% of the nanoparticle catalyst is, the more intensified is the result with an amount of 5 wt%.

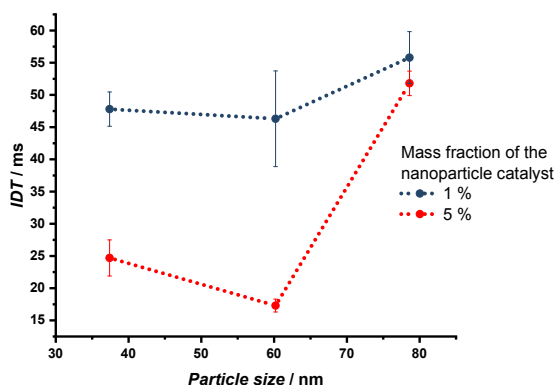


Figure 8: IDTs which were accomplished with the bipropellant TMEDA/HTP in dependency of silver nanoparticles of different sizes at catalysts in different percentages.

Figure 8 shows that the shortest IDTs were measured with the medium sized silver nanoparticles. It is therefore assumed, that size of nanoparticles is not the only key element in finding a beneficial catalyst. The medium sized silver nanoparticles were synthesised using the citrate method, where the sodium citrate used in this synthesis serves both as reducing and capping agent. After synthesis and purification, capping agents typically remain as surround on



the surface of the nanoparticles and function as stabilisers. The amount of this residue was determined throughout thermogravimetry (TG) combined with differential scanning calorimetry (DSC). As stated in table 1, the amount of the capping agent varies widely between the different silver nanoparticles, as they were synthesised by different methods. The medium sized nanoparticles possess the largest amount of remaining capping agent by far (almost 31 wt%, Fig. 9, left side). In contrast to that, the other silver nanoparticles show much less capping agent: 0.42 wt% (Fig. 9, right side) in case of the smallest particles synthesised with the polyol method and almost 3 wt% (Tab. 1) for the largest particles synthesised by reduction with glucose.

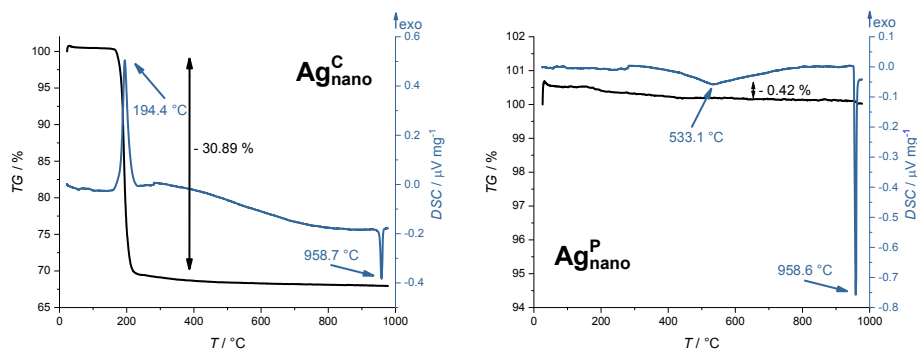


Figure 9: Thermogram and DSC curve of  $\text{Ag}_{\text{nano}}^{\text{C}}$  and  $\text{Ag}_{\text{nano}}^{\text{P}}$ . The measurements were carried out in a sample crucibles made of aluminium oxide under nitrogen.

This finding leads us to the following conclusions:

- First, a large amount of capping agent may have a positive impact on the catalyst effect of the nanoparticles. This observation will be studied subsequently.
- Second, a better comparison as to the influence of the nanoparticle size is possible between  $\text{Ag}_{\text{nano}}^{\text{P}}$  and  $\text{Ag}_{\text{nano}}^{\text{G}}$ . On the surface of these two kinds of particles, a similar amount of stabilising capping agents is remaining. The consideration of results obtained with the propellants containing these two kinds of particles show, that the average IDT of the fuel containing smaller silver nanoparticles is significantly shorter. This result can be explained by the higher surface to volume ratio of smaller particles. As the surface area is the catalytically active area of a compound, this finding was to be expected.

In total, the dependency of the particle sizes as to their catalyst properties was found. But particle size seems not to be the only crucial factor, so other influences have to be further investigated.

### 3.3.5 Test series 4: Impact of additional stabilisers

The effect of the addition of stabilising capping agent to the nanoparticle catalysts is investigated in test series 4. As the smaller  $\text{Ag}_{\text{nano}}^{\text{P}}$  achieved better results than the  $\text{Ag}_{\text{nano}}^{\text{G}}$  in the former tests, the first-mentioned were utilised for the following tests. 0,42 wt% of capping agent PVP ( $M_w = 2\,500\text{ g/mol}$ ) remained as a residue on the surface of these silver particles. But as this residue couldn't be prevented by the wet chemical procedures, it was accepted, but will be neglected in the further research.

To investigate the influence of the capping agents, the stabilising ligands sodium citrate and PVP ( $M_w = 2\,500\text{ g/mol}$ ) were added to the  $\text{Ag}_{\text{nano}}^{\text{P}}$ . Both capping stabilisers were tested, in order to clarify if the  $\text{Ag}_{\text{nano}}^{\text{C}}$  showed better performance upon the citrate or the large amount of capping agent in general. The percentage of the additives was set to 10 wt% or 30 wt% respectively. Directly after synthesis and purification of the nanoparticles, a dispersion was prepared via an ultrasonic probe. Ethanol was used as dispersant.

Initially, evenly distributed dispersions of all samples were produced by ultra-sonification. But large differences were visible after 24 hours. As the photograph on the left side of figure 10 shows, the dispersions with added citrate were still highly homogenous, while the particles in the dispersion with added PVP settled down (photograph on the right side).

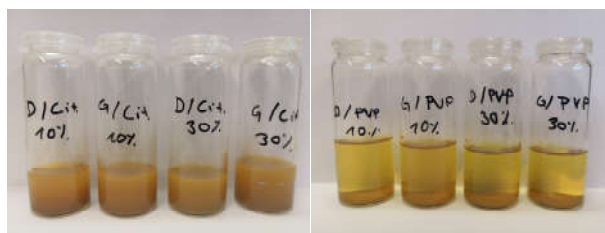


Figure 10: Comparison of the dispersions of  $\text{Ag}_{\text{nano}}^{\text{P}}$  in Ethanol after 24 hours. Left side: with 10 wt% or 30 wt% citrate stabilised dispersions. Right side: with 10 wt% or 30 wt% PVP stabilised dispersions. [20]

Now, TMEDA gels were produced out of the different stabilised nanoparticles with 10 wt% or 30 wt% additional sodium citrate or PVP. The results of the performed drop-on-pool tests are summarised in table 5.

Table 5: Parameters of test series 4 with average IDTs and respective standard deviations.

Catalyst	Amount of catalyst [wt%]	Condition of the nanoparticles	Number of tests	Average IDT [ms]	Standard deviation [ms]
$\text{Ag}_{\text{nano}}^{\text{P}}$ (10 wt% PVP)	5	dried	2	51.1	4.3
$\text{Ag}_{\text{nano}}^{\text{P}}$ (30 wt% PVP)	5	dried	2	55.3	8.0
$\text{Ag}_{\text{nano}}^{\text{P}}$ (10 wt% citrate)	5	dried	2	23.4	0.4
$\text{Ag}_{\text{nano}}^{\text{P}}$ (30 wt% citrate)	5	dried	2	24.0	0.3

Test series 4 shows a clear trend: while the propellants with PVP stabilised nanoparticles had a much worse performance, citrate stabilised nanoparticles are slightly advantageous compared to the reference value without stabiliser. Figure 11 demonstrates the findings of test series 4.

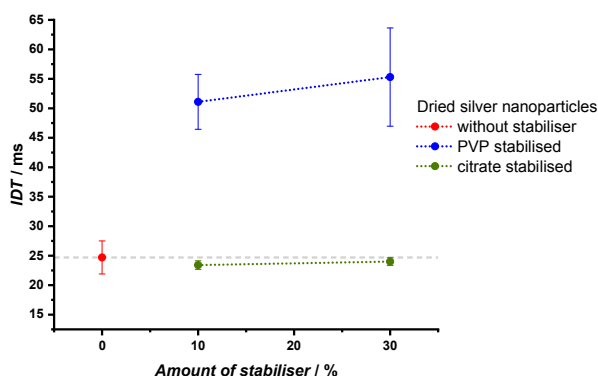


Figure 11: IDTs which were accomplished with the bipropellant TMEDA/HTP with 5 wt% dried  $\text{Ag}_{\text{nano}}^{\text{P}}$  as catalyst in dependency of added capping agents.

Figure 11 highlights that the IDTs are slowed down clearly upon the addition of PVP. The settling of the particles in figure 10 indicates that PVP does not have a stabilising effect on the dispersions. In fact, they even seem to inhibit the catalytic activity of the nanoparticles, as the nanoparticles stabilised with 30 wt% PVP show even worse results than those stabilised with 10 wt% PVP. In contrast to that, slightly shorter IDTs were obtained through the addition of citrate. Even though the degree of this improvement is very small at this point, this observation will be important for the further procedure.

### 3.3.6 Test series 5: Different states of the nanoparticles (dried or dispersed in ethanol).

In test series 5, a new approach was adopted to improve the catalytic activity of the nanoparticles. During the drying of nanoparticle dispersions, agglomerates are formed. In order to obtain a fuel with finely distributed nanoparticles, the nanoparticles were not dried, but were used as dispersion in a residue of ethanol. Due to the fact that alcohols are not basic, they are not well suited as hypergolic fuels in combination with HTP in general. Despite that fact, this test series will check if this disadvantage can be compensated by prevention of agglomeration of the nanoparticles and thus, a greater surface area that is catalytically active. The amount of ethanol in these fuels amounted to 5 wt%.

The first stage, test series 5a, involves the repetition of test series 2 with the changes explained above. So the silver nanoparticles, which were dispersed in ethanol, were added as catalyst to the fuel. Table 6 comprises the results of test series 5a.

Table 6: Parameters of test series 5a with average IDTs and respective standard deviations.

Catalyst	Average particle size (DLS) [nm]	Amount of catalyst [wt%]	Condition of the nanoparticles	Number of tests	Average IDT [ms]	Standard deviation [ms]
$\text{Ag}_{\text{nano}}^{\text{P}}$	37.4	1	Dispersion (EtOH)	3	31.7	1.7
$\text{Ag}_{\text{nano}}^{\text{C}}$	60.2	1	Dispersion (EtOH)	3	18.0	0.8
$\text{Ag}_{\text{nano}}^{\text{G}}$	78.6	1	Dispersion (EtOH)	3	51.2	15.8

Furthermore, table 7 compares the respective results of test series 2 and 5a.

Table 7: Comparison of IDTs of test series 2 and 5a. For all values applies: amount of catalyst: 1 wt%, number of tests: 3.

Catalyst	Average particle size (DLS) [nm]	Average IDT [ms] dried particles	Average IDT [ms] dispersion (EtOH)
$\text{Ag}_{\text{nano}}^{\text{P}}$	37.4	47.8	31.7
$\text{Ag}_{\text{nano}}^{\text{C}}$	60.2	46.4	18.0
$\text{Ag}_{\text{nano}}^{\text{G}}$	78.6	55.8	51.2

The results presented in table 7 show a distinct improvement of the average IDTs. Again, the degree of the improvement varies between different silver nanoparticle catalysts. But overall, the usage of undried nanoparticles seems to have a positive impact on the catalysts performance. In figure 12, the average IDTs of the two test series 2 and 5a are compared. The grey curve shows the IDTs which were accomplished with dried nanoparticles, the orange curve those of nanoparticles dispersed in a residue of ethanol. It is conspicuous that the curve progression is similar to that in figure 8, where different amounts of the catalysts are compared. In both cases, the improvement varies, as the better it was initially, the more it could be improved.

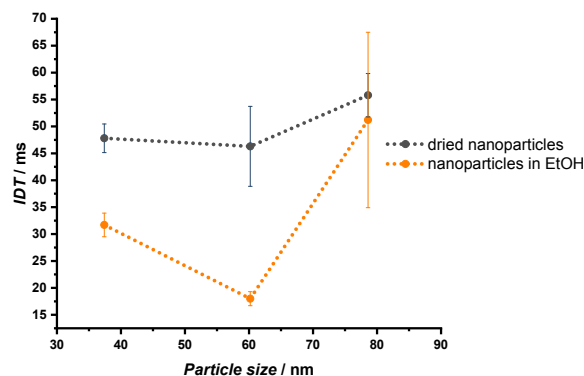


Figure 12: IDTs which were accomplished with the bipropellant TMEDA/HTP with 1 wt% silver nanoparticles of different sizes as catalysts

As the former attempt has been successful, the parameters of test series 4 were also picked up again with the pertinent change. Table 8 lists the data of this test series 5b:

Table 8: Parameters of test series 5b with average IDTs and respective standard deviations.

Catalyst	Amount of catalyst [wt%]	Condition of the nanoparticles	Number of tests	Average IDT [ms]	Standard deviation [ms]
<b>Ag<sub>nano</sub><sup>P</sup> (10 wt% PVP)</b>	5	Dispersion (EtOH)	2	45.7	1.3
<b>Ag<sub>nano</sub><sup>P</sup> (30 wt% PVP)</b>	5	Dispersion (EtOH)	2	51.4	0.7
<b>Ag<sub>nano</sub><sup>P</sup> (10 wt% citrate)</b>	5	Dispersion (EtOH)	3	8.8	1.0
<b>Ag<sub>nano</sub><sup>P</sup> (30 wt% citrate)</b>	5	Dispersion (EtOH)	2	18.9	2.2

Also, in table 9 the results of test series 5b are contrasted with those of test series 4:

Table 9: Comparison of IDTs of test series 4 and 5b. For all values applies: amount of catalyst: 5 wt%, number of tests: 2 (3 for Ag<sub>nano</sub><sup>P</sup> (10 wt% citrate)).

Catalyst	Average IDT [ms] dried particles	Average IDT [ms] dispersion (EtOH)
<b>Ag<sub>nano</sub><sup>P</sup> (10 wt% PVP)</b>	51.1	45.7
<b>Ag<sub>nano</sub><sup>P</sup> (30 wt% PVP)</b>	55.3	51.4
<b>Ag<sub>nano</sub><sup>P</sup> (10 wt% citrate)</b>	23.4	8.8
<b>Ag<sub>nano</sub><sup>P</sup> (30 wt% citrate)</b>	24.0	18.9

In figure 13, the average ignition delay times of these different propellants are demonstrated. In the same way as in test series 5a, the IDTs could be shortened through substitution of dried nanoparticles with undried ones in all cases. Again, the deterioration of fuels containing nanoparticles with added PVP is due to the fact, that the stabilisation provided through PVP is very low (Fig. 10). In contrast, citrate stabilised nanoparticles show an increased catalytic activity, which is further improved through the use of nanoparticles dispersed in ethanol. To verify the role of citrate as stabilising capping agent, the zeta potential of the  $\text{Ag}_{\text{nano}}^{\text{P}}$  stabilised with 10 wt% citrate was measured. The measured value  $\zeta = -38.47$  mV is almost twice as high as the value of the  $\text{Ag}_{\text{nano}}^{\text{P}}$  without stabilisation ( $\zeta = -21.73$  mV). So, the electrostatic stabilisation of the particles is increased through the addition of citrate to the dispersion in ethanol. This stabilisation has a positive impact on the catalytic activity of the nanoparticles. It should be assumed, that this leads to the prevention of aggregation and is related to finer distribution of the nanoparticles in TMEDA. The outcome is a higher catalytic activity of the nanoparticles, as the non-agglomerated particles have a higher surface to volume ratio and are therefore more reactive. It can be excluded that sodium citrate itself is responsible for the improved results, as sodium citrate and HTP do not chemically react with each other.

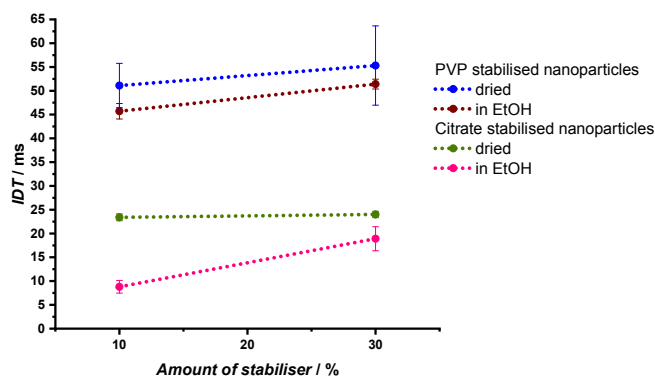


Figure 13: IDTs which were accomplished with the bipropellant TMEDA/HTP with 5 wt%  $\text{Ag}_{\text{nano}}^{\text{P}}$  as catalysts in dependency of added capping agents.

The key step for the optimal utilization of nanoparticles is, to reach the best possible distribution and prevent the formation of agglomerates. Both PVP and citrate stabilised nanoparticles showed better performances with undried particles than with dried ones. The comparison of the amount of stabiliser shows, that in general with a mass fraction of 10 wt% stabiliser shorter ignition delay times are accomplished than with 30 wt%. Therefore a smaller quantity of the capping agent is enough to ensure stabilisation; larger amounts seem obstructive. Through comprehensive variation of the percentage of the capping agent, this aspect could be further optimised.

As a whole, the shortest average IDT of  $8.8 \text{ ms} \pm 1.0 \text{ ms}$  was measured for a fuel containing 5 wt% silver nanoparticles dispersed in ethanol as catalyst, which were stabilised with 10 wt% of sodium citrate. As a whole, the different improvements lead to a significantly optimisation of the results and therefore to a sustainable hypergolic propellant. Figure 14 shows sequences of the overall shortest measurement.

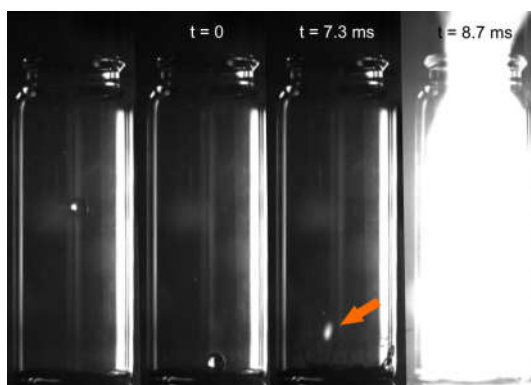


Figure 14: Sequences of the high-speed video of the fuel, which achieved the shortest IDT. [20]

#### 4. Conclusion and Outlook

The aim of this work was the creation of new “green” hypergolic propellants with nanoparticles as catalysts. After the choice of suitable nanoparticles, different syntheses were carried out and nanoparticles were completely characterised. Gelled fuels containing these nanoparticles were produced on basis of TMEDA. Through the implantation of drop-on-pool tests, ignition delay times were investigated as a measure for a performance parameter of the hypergolic propellants with HTP as oxidiser.

Different test series were carried out to optimise the system with the aim of decreasing the IDT.

- First, the different nanoparticles (Ag, Pt, MnO<sub>2</sub>) were tested with the outcome, that silver nanoparticles showed the best results.
- Further investigation was made as to the size of the nanoparticles, only using silver.
- Moreover, the influence of different capping agents was tested, which lead to a better stabilisation of the nanoparticles.
- Additionally, the IDT was shortened by introducing nanoparticles in the fuel as dispersion with a residue of ethanol instead of drying them.

In this way, an optimised propellant was created which achieved an average ignition delay time of 8.8 ms ± 1.0 ms. This not only meets the requirement of an acceptable fuel, but also the criteria for one with a preferred performance, because it falls below the benchmark of 10 ms. From this point of view, this green propellant is able to keep up with common toxic hypergolic bipropellants.

Considering future work, even smaller nanoparticles could be tested as catalysts. It is to be expected that smaller particles would lead to enhanced performances or a smaller amount of catalyst would be required for similar findings. Moreover, the investigation of other metal or metal oxide nanoparticles could be interesting. In this way, tailor-made nanoparticles could be designed for individual requirement of different propellants. Furthermore, other organic liquids as basis of the gelled propellants could be utilised instead of TMEDA. Another aspect could be the increase of the catalysts percentage, which would probably lead to shorter IDTs. But a higher amount of catalyst also involves disadvantages as higher costs and impairs fuel performance; therefore this approach was rejected here.

#### 5. Acknowledgement

The authors would like to thank the M11 test bench team for the support, especially Nicole Röcke for her support in the physical-chemical laboratory. Furthermore we would like to thank Johannes Stadtmüller und Stefan Belle from the University of Applied Sciences Aschaffenburg for providing assistance in EDX-analysis.

#### References

- [1] Florczuk, W. and G. Rarata. 2015. Assesment of various fuel additives for reliable hypergolic ignition with HTP. In: *66th International Astronautical Congress*.
- [2] Hydrazine REACH Authorisation Task Force of the European Space Industry. *Position Paper; Exemption of propellant-related use of hydrazine from REACH authorisation requirement*. ASD Eurospace.
- [3] Jyoti, B. V. S., M. S. Naseem and S. W. Baek. 2017. Hypergolicity and ignition delay study of pure and energized ethanol gel fuel with hydrogen peroxide. *Combust. Flame*, 176:318–325.
- [4] Frolik, S., B. Austin, J. Rusek and S. Heister. 2000. Development of hypergolic liquid fuels for use with hydrogen peroxide. In: *36th AIAA/ASME/SAE/ASEE Joint Propulsion Conference and Exhibit*.
- [5] W Florczuk, W. and G. Rarata. 2017. Performance evaluation of the hypergolic green propellants based on the HTP for a future next generation spacecrafts. In: *53rd AIAA/SAE/ASEE Joint Propulsion Conference*.
- [6] Kirchberger, C. U., P. Kröger, M. Negri and H. K. Ciezki. 2016. Overview on the Gelled Propellants Activities of DLR Lampoldshausen. In: *52nd AIAA/SAE/ASEE Joint Propulsion Conference*.
- [7] Kurilov, M., C. Kirchberger, D. Freudenmann, A. Stiefel and H. K. Ciezki. 2018. A Method for Screening and Identification of Green Hypergolic Bipropellants. *Int. J. Energ. Mater. Chem. Prop.* 17(3): 183–203.
- [8] Keese, D. L., B. M. Melof, B. V. Ingram, W. R. Escapule, M. C. Grubelich and J. Ruffner. 2004. Hydrogen Peroxide-Based Propulsion and Power Systems. *Sandia National Laboratories*.
- [9] Holleman, A. F., E. Wiberg and N. Wiberg. 1995. *Lehrbuch der Anorganischen Chemie*. Gruyter. ISBN: 978-3110126419.
- [10] Palmer, R. K. and J. J. Russel. 2004. Low Toxicity Reactive Hypergolic Fuels for Use with Hydrogen Peroxide. In: *Proceedings of the 2nd International Conference on Green Propellants for Space Propulsion*.
- [11] GESTIS substance database. 19.02.2019. Entry for *N,N,N',N'-Tetramethylenethyldiamin*.
- [12] Shvets, G. 2008. Metamaterials add an extra dimension. *Nat. Mater.* 7(1):7–8.

- [13] Wedler, G. and H.-J. Freund. 2012. *Lehrbuch Der Physikalischen Chemie*. Wiley-VCH Verlag GmbH. ISBN: 978-3527329090.
- [14] Boström, M., D. R. M. Williams and B. W. Ninham. 2001. Specific Ion Effects: Why DLVO Theory Fails for Biology and Colloid Systems. *Phys. Rev. Lett.* 87(16):168103.
- [15] Israelachvili, J. N. *Van der Waals Forces. Intermolecular and Surface Forces*. 2011. Elsevier. ISBN: 9780123919274.
- [16] Atkins P. and J. de Paula. *Physical Chemistry*, 9th Edition. 2009. Oxford University Press, ISBN: 1429218126.
- [17] Kirby, B. J. and E. F. Hasselbrink. 2004. Zeta potential of microfluidic substrates: 1. Theory, experimental techniques, and effects on separations. *Electrophoresis*. 25(2):187–202.
- [18] Dörfler, H.-D. 2002. *Grenzflächen und kolloid-disperse Systeme*. Springer-Verlag, ISBN: 3540425470.
- [19] Fritz, G., V. Schädler, N. Willenbacher and N. J. Wagner. 2002. Electrosteric Stabilization of Colloidal Dispersions. *Langmuir*. 18:6381–6390.
- [20] Ricker, S. 2019. *Hypergolisierung von Geltreibstoffen mit Hilfe von Nanopartikeln*. Master's Thesis. DLR, Institute of Space Propulsion, Lampoldshausen; University of Würzburg, Institute of Physical and Theoretical Chemistry.
- [21] Kim, D., S. Jeong und J. Moon. 2006. Synthesis of silver nanoparticles using the polyol process and the influence of precursor injection. *Nanotechnology*. 17(16): 4019–4024.
- [22] Kittler, S., C. Greulich, J. S. Gebauer, J. Diendorf, L. Treuel, L. Ruiz, J. M. Gonzalez-Calbet, M. Vallet-Regi, R. Zellner, M. Köller und M. Epple. 2010. The influence of proteins on the dispersability and cell-biological activity of silver nanoparticles. *J. Mater. Chem.* 20(3):512–518.
- [23] Helmlinger, J., C. Sengstock, C. Groß-Heitfeld, C. Mayer, T. A. Schildhauer, M. Koeller und M. Epple. 2016. Silver nanoparticles with different size and shape: equal cytotoxicity, but different antibacterial effects. *RSC Adv.* 6 (22):18490–18501.
- [24] Bonet, F., V. Delmas, S. Grugeon, R. H. Urbina, P.-Y. Silvert und K. Tekaia-Elhsissen. 1999. Synthesis of monodisperse Au, Pt, Pd, Ru and Ir nanoparticles in ethylene glycol. *Nanostruct. Mater.* 11(8), 1277–1284.
- [25] Neelam, M. Kumar und G. Rani. 2017. Green Route for the Synthesis of Manganese Oxide Nanoparticles by Co-precipitation Method. In: *International Conference on Recent Innovations in Science, Engineering and Technology*. 1006–1009.
- [26] Zhang, Y., H. Gao, Y.-H. Joo, and J. M. Shreeve. 2011. Ionic Liquids as Hypergolic Fuels. *Angew. Chem. Int. Ed.* 50:9554–9562.